Doping dependent isotope effects of the quasi-1D electron-phonon system: comparison with the high-temperature superconductors

I. P. Bindloss
Department of Physics, University of California, Los Angeles, California 90095–1547
(Dated: February 2, 2008)

The weak-coupling quantum phase diagrams of the one-dimensional (1D) Holstein-Hubbard and Peierls-Hubbard models are computed near half-filling, using a multi-step renormalization group technique. If strong enough, the electron-phonon interaction induces a spin gap. The spin gap, which determines the superconducting pairing energy, depends strongly on the band filling and decreases monotonically as the system is doped away from half-filling. However, the superconducting susceptibility exhibits a different doping dependence; it can vary non-monotonically with doping and exhibit a maximum at an "optimal" value of the doping. For a quasi-1D array of weakly coupled, fluctuating 1D chains, the superconducting transition temperature T_c exhibits a similar non-monotonic doping dependence. The effect of changing the ion mass (isotope effect) on T_c is found to be largest near half-filling and to decrease rapidly upon doping away from half-filling. The isotope effect on the spin gap is the opposite sign as the isotope effect on T_c. We discuss qualitative similarities between these results and properties of the high-temperature superconductors.

Recent experiments in the high-temperature superconductors suggest the presence of a strong, ubiquitous, yet unconventional electron-phonon (el-ph) interaction [1, 2]. It has been known for some time that these materials exhibit large and strongly doping dependent oxygen isotope effects [3, 4, 5] that cannot be described with the conventional BCS theory used for ordinary metals. In this Letter, we show that the quasi-1D electron gas coupled to phonons exhibits highly unconventional doping dependent isotope effects that are qualitatively similar to those observed in the high-temperature superconductors.

The best understood non-Fermi liquid is the spin-charge separated one-dimensional electron gas (1DEG) [6]. The properties of the 1DEG coupled to phonons are dramatically different from a conventional metal coupled to phonons [7, 8, 9, 10]. Unlike in a Fermi liquid, in 1D the el-ph interaction is strongly renormalized, and the renormalization is strongly affected by direct electron-electron (el-el) interactions. Due to these renormalization effects, a weak, retarded el-ph interaction is capable of inducing a spin gap and causing a divergent superconducting susceptibility, even when the el-el repulsion is the dominant microscopic interaction [9]. Unlike the case in 3D, in 1D this can occur without a large amount of retardation. In contrast to BCS theory, the pairing energy and superconducting susceptibility are very sensitive to the band filling.

In the cuprates, both the superconducting transition temperature T_c and the isotope effect exponent $\alpha_{T_c} = -d\ln T_c/d\ln M$, which describes changes in T_c induced by changes in the oxygen mass M, exhibit highly unconventional (*i.e.* non-BCS) doping dependencies. In BCS theory, T_c is only weakly dependent on the carrier concentration, and α_{T_c} has the universal value of $1/2$. In the cuprates, T_c exhibits a maximum as a function of doping, and the isotope effect is not universal–it is strongly doping and somewhat material dependent. For the underdoped cuprates, $\alpha_{T_c} \approx 1$ (indicating that, at least in this region, phonons play an important role in the superconductivity). As the doping increases, α_{T_c} decreases, usually dropping below 0.1 near optimal doping [3]. The origin of this behavior remains a mystery of high-T_c superconductivity that any successful microscopic theory of pairing should explain. Below we provide a microscopic theory that is capable of rationalizing it.

In this Letter, we compute α_{T_c} for a quasi-1DEG coupled to phonons, under the assumption that charge density wave (CDW) order is dephased by spatial or dynamic fluctuations of the 1D chains [11, 12]. For many choices of the parameters, α_{T_c} is larger than the BCS value at small dopings, then drops below the BCS value as the doping is increased – the same behavior observed in the cuprate superconductors. We show that the quasi-1DEG coupled to phonons displays a strongly doping dependent T_c that can exhibit a maximum as a function of doping. This behavior occurs despite the fact that the pairing energy, determined by the spin gap Δ_s, is a monotonically decreasing function of increasing doping. We also compute the isotope exponent $\alpha_{\Delta_s} = -d\ln\Delta_s/d\ln M$. We find $\alpha_{\Delta_s} < 0$, the same sign as the isotope effect observed on the pseudogap temperature in the cuprates [4].

The technique we employ is the multi-step renormalization group (MSRG) method described in detail in a previous paper [9]. This method treats el-el and el-ph interactions on equal footing and properly treats the quantum phonon fluctuations. In it, we start with a microscopic el-ph model and integrate out high energy degrees of freedom, via an RG transformation. This is done in multiple steps, as elaborated below. At low energies one obtains an effective field theory that is the same as the ordinary 1DEG, except for phonon induced renormalizations of the el-el interactions and bandwidth. The accuracy of this analytic technique in computing weak-coupling phase diagrams was demonstrated in Ref. 9 by

comparison with exact numerical results. We shall apply it to two models of interacting, spinful 1D electrons coupled to phonons:

The 1D Peierls-Hubbard (Pei-Hub) Hamiltonian is

$$\mathcal{H}_{\rm Pei-Hub} = -\sum_{i,\sigma}\left[t-\gamma(u_{i+1}-u_i)\right](c^\dagger_{i,\sigma}c_{i+1,\sigma}+{\rm H.C.}) + \sum_i\left[\frac{p_i^2}{2M}+\frac{\kappa}{2}(u_{i+1}-u_i)^2\right]+U\sum_i n_{i,\uparrow}n_{i,\downarrow}\,.$$

In this model, acoustic phonons couple to electrons by modifying the bare hopping matrix element t by the el-ph coupling strength γ times the relative displacements $u_{i+1}-u_i$ of two neighboring ions [13]. The last term is the Hubbard interaction. For this model, we shall approximate the phonon dispersion by its value at the zone boundary of $2\sqrt{\kappa/M}\equiv\omega_0$, since the el-ph interaction vanishes at zero momentum transfer.

The 1D Holstein-Hubbard (Hol-Hub) Hamiltonian is

$$\mathcal{H}_{\rm Hol-Hub} = -t\sum_{i,\sigma}(c^\dagger_{i,\sigma}c_{i+1,\sigma}+{\rm H.C.})+\sum_i\left[\frac{p_i^2}{2M}+\frac{K}{2}q_i^2\right] + g\sqrt{2M\omega_0}\sum_i q_i n_i + U\sum_i n_{i,\uparrow}n_{i,\downarrow}\,.$$

Here dispersionless optical phonons with coordinate q_i and frequency $\omega_0=\sqrt{K/M}$ couple to the electron density $n_i=\sum_\sigma c^\dagger_{i,\sigma}c_{i,\sigma}$ with el-ph coupling strength g [14].

It is convenient to define the dimensionless quantities

$$\lambda_{\rm Pei}=2N_0(\gamma\sin k_F)^2/\kappa\,,\quad \lambda_{\rm Hol}=N_0g^2/\omega_0\,,$$
$$\bar U=U/(\pi v_F)\,,\quad \delta=\ln(\mu/\omega_0)/\ln(E_F/\omega_0)\,,$$

where $N_0\equiv 2/(\pi v_F)$. As usual, v_F, k_F, and E_F are the Fermi velocity, momentum, and energy, respectively. (We have set $\hbar$ and the lattice parameter equal to unity.) μ is the chemical potential measured with respect to its value at half-filling. In this Letter, we study the range $\omega_0<\mu<E_F$ ($0<\delta<1$). The doping concentration relative to half-filling is given by $x\approx N_0\omega_0(E_F/\omega_0)^\delta$. Since the MSRG method is perturbative, it is only quantitatively accurate for $\lambda_\nu,\bar U\ll 1$, but is believed to be qualitatively accurate for $\lambda_\nu,\bar U\lesssim 1$ [9]. (The subscript ν stands for Pei or Hol.)

Fig. 1 presents the $\lambda_\nu-\delta$ phase diagrams of the above models, computed with MSRG for several fixed values of $\bar U$. The phase boundaries separate regions where various types of order have divergent susceptibilities in the low temperature limit. The susceptibility that diverges most strongly (*i.e.* dominates) is shown without parenthesis; parenthesis indicate a susceptibility that diverges less strongly. The charge sector is gapless everywhere in the phase diagrams. Above the thick solid line, the system is spin-gapped and described as a Luther-Emery liquid (LEL) [15]. Below this line, it is a gapless, quantum-critical Luttinger liquid (LL) [6].

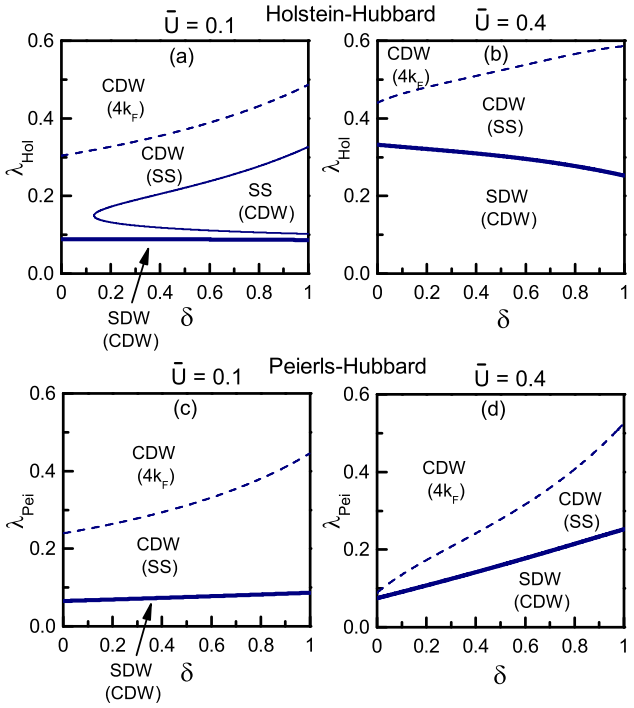

FIG. 1: $T=0$ phase diagrams for the Hol-Hub model (panels a and b), and Pei-Hub model (panels c and d). (a) and (c) are for $\bar U=0.1$; (b) and (d) are for $\bar U=0.4$. For all diagrams, $E_F/\omega_0=5$. Parenthesis indicate a sub-dominant susceptibility. SDW stands for $2k_F$ spin density wave, CDW stands for $2k_F$ charge density wave, SS stands for singlet superconductivity, and $4k_F$ stands for $4k_F$ charge density wave.

The thick solid line in Fig. 1 is determined by integrating out degrees of freedom between E_F and ω_0, and then requiring that the total effective backward-scattering interaction $g_1^{\rm tot}(\omega_0)=\bar U/(1+\bar U l_0)-\lambda_1(\omega_0)$ is zero. Here $l_0\equiv\ln(E_F/\omega_0)$ and $\lambda_1(\omega_0)>0$ is the effective strength of the backward scattering (momentum transfer near $2k_F$) portion of the el-ph interaction. Below the thick line in Fig. 1, $g_1^{\rm tot}(\omega_0)>0$ and the RG flows carry the effective $g_1^{\rm tot}$ to zero at low energies, signifying the stability of the LL fixed point. Above the thick line, $g_1^{\rm tot}(\omega_0)<0$ and the RG flows carry $g_1^{\rm tot}$ to minus infinity at low energies, indicating the existence of a spin gap.

$\lambda_1(\omega_0)$ is determined in two steps: First, one integrates from E_F to μ using the RG flow equations that govern half-filled systems, resulting in an effective λ_1 of [9]

$$\lambda_1(\mu)=\left(\frac{\lambda_{\rm Hol}}{1-\lambda_{\rm Hol}X/\bar U}\right)\sqrt{\frac{1-c\bar U l_0}{(1+c\bar U l_0)^3}} \qquad (1)$$

or

$$\lambda_1(\mu)=\left(\frac{\lambda_{\rm Pei}}{1-\lambda_{\rm Pei}Y/\bar U}\right)\sqrt{\frac{1}{[1-(c\bar U l_0)^2]^3}} \qquad (2)$$

for the Hol-Hub and Pei-Hub models respectively, where $X\equiv 4\left[1-\sqrt{(1-c\bar U l_0)/(1+c\bar U l_0)}\right]-2\arcsin(c\bar U l_0)$,

$Y \equiv 2c\bar{U}l_0/\sqrt{1-(c\bar{U}l_0)^2}$, and $c \equiv 1-\delta$. Next, $\lambda_1(\mu)$ is used as the initial value to integrate from μ to ω_0, employing the RG flow equations that govern incommensurate systems, resulting in [9]

$$\lambda_1(\omega_0) = \left(\frac{\lambda_1(\mu)}{1-\lambda_1(\mu)Z/\bar{U}}\right)\sqrt{\frac{\exp(\delta\bar{U}l_0)}{(1+\delta\bar{U}l_0)^3}} \qquad (3)$$

for either model, where $Z \equiv \int_0^{\delta\bar{U}l_0} du\sqrt{\exp(u)/(1+u)^3}$. The condition $g_1^{\rm tot}(\omega_0)=0$ then determines the following critical values for the microscopic el-ph couplings:

$$\lambda_{\rm Hol}^{\rm Gap} = \bar{U}\left\{\left[(1+\bar{U}l_0)S_3+Z\right]/S_1+X\right\}^{-1}, \qquad (4)$$

$$\lambda_{\rm Pei}^{\rm Gap} = \bar{U}\left\{\left[(1+\bar{U}l_0)S_3+Z\right]/S_2+Y\right\}^{-1}, \qquad (5)$$

where we defined $S_1 = (1+c\bar{U}l_0)^{3/2}(1-c\bar{U}l_0)^{-1/2}$, $S_2 = \left[1-(c\bar{U}l_0)^2\right]^{3/2}$, and $S_3 = e^{\delta\bar{U}l_0/2}(1+\delta\bar{U}l_0)^{-3/2}$. The system is a spin-gapped LEL for $\lambda_\nu > \lambda_\nu^{\rm Gap}$.

In the LEL phase, the portion of the singlet superconductivity (SS) and $2k_F$ CDW susceptibility that is potentially strongly divergent as $T\to 0$ is given by $\chi_{\rm SS} = (\pi v_F)^{-1}(\Delta_s/E_F)(T/E_F)^{1/K_c^{\rm eff}-2}$ and $\chi_{\rm CDW} = (\pi v_F)^{-1}(\Delta_s/E_F)(T/E_F)^{K_c^{\rm eff}-2}$ respectively, where the spin gap is $\Delta_s = \omega_0 e\exp[-1/|g_1^{\rm tot}(\omega_0)|]$ [9], and the effective charge Luttinger exponent after integrating out states between E_F and ω_0 is $K_c^{\rm eff} = \sqrt{[2+2g_4^{\rm tot}+g_c^{\rm tot}(\omega_0)]/[2+2g_4^{\rm tot}-g_c^{\rm tot}(\omega_0)]}$. Here $g_c^{\rm tot}(\omega_0) = g_c^{\rm el}(\mu)-\lambda_1(\omega_0)+2\lambda_2$ and $g_4^{\rm tot} = \bar{U}/2-\lambda_2$, where the forward scattering el-ph interaction λ_2 is given by $\lambda_2 = \lambda_{\rm Hol}$ for the Hol-Hub model and $\lambda_2 = 0$ for the Pei-Hub model. The contribution of the Hubbard interaction to $g_c^{\rm tot}(\omega_0)$, given by $g_c^{\rm el}(\mu) = -\bar{U}/(1-c\bar{U}l_0)$, is obtained by integrating out states between E_F and μ, since this contribution is unrenormalized below μ. Note that $K_c^{\rm eff}$ is the effective value at low energies because $g_c^{\rm tot}$ is not further renormalized below ω_0 [16].

The SS susceptibility is the dominant one if $K_c^{\rm eff} > 1$. The thin solid line in Fig. 1a is the critical line determined by $K_c^{\rm eff}=1$, given by

$$\lambda_{\rm Hol}^{\rm SS,\pm} = \bar{U}\left[B \pm \sqrt{B^2 - S_1AC/2}\right], \qquad (6)$$

where $A = (S_1X+Z)^{-1}$, $B = [(2S_1-S_3)A+C]/4$, and $C = (1-c\bar{U}l_0)^{-1}$. $\chi_{\rm SS}$ is dominant if the two conditions $S_1AC < 2B^2$ and $\lambda_{\rm Hol}^{\rm SS,-} < \lambda_{\rm Hol} < \lambda_{\rm Hol}^{\rm SS,+}$ are met. The thin solid line is absent in Fig. 1b because $S_1AC > 2B^2$ everywhere. This line is never present in the Pei-Hub model with $\bar{U} > 0$, because then $K_c^{\rm eff} < 1$ always.

For $1/2 < K_c^{\rm eff} < 1$, $\chi_{\rm SS}$ is still divergent as $T\to 0$, but, for a single chain 1DEG, $\chi_{\rm CDW}$ is more strongly divergent. The dashed lines in Fig. 1 are determined by $K_c^{\rm eff} = 1/2$, which leads to the following critical values for the microscopic el-ph interactions

$$\lambda_{\rm Hol}^{\rm CDW} = \bar{U}\left[D+\sqrt{D^2+5S_1AE/4}\right], \qquad (7)$$

$$\lambda_{\rm Pei}^{\rm CDW} = \bar{U}\left[(S_3/E+Z)/S_2+Y\right]^{-1}, \qquad (8)$$

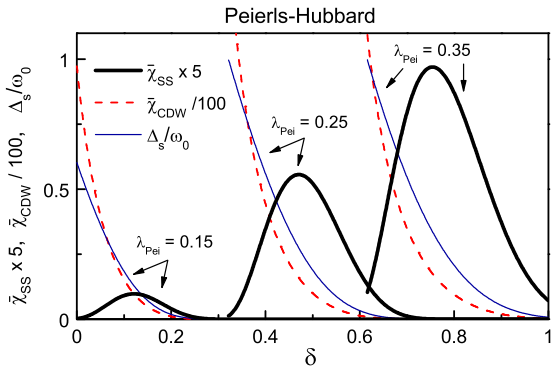

FIG. 2: Doping dependence of the dimensionless singlet superconducting susceptibility $\bar{\chi}_{\rm SS}$ (thick solid lines), CDW susceptibility $\bar{\chi}_{\rm CDW}$ (dashed lines), and spin gap (thin solid lines), for the Pei-Hub model with $\bar{U}=0.4$, $E_F/\omega_0=5$, and various values of $\lambda_{\rm Pei}$ (labeled in plot). $\bar{\chi}_{\rm SS}$ and $\bar{\chi}_{\rm CDW}$ were computed for $T/\omega_0 = 0.1$.

where $D = A[S_1(4-5EX)-5(EZ+S_3)]/8$ and $E = (6/\bar{U}+3)/5-C$. If $\lambda_\nu > \lambda_\nu^{\rm CDW}$, then $K_c^{\rm eff} < 1/2$, which means that SS is not divergent.

Examining Fig. 1d, we see that for moderate values of $\lambda_{\rm Pei}$, for example near $\lambda_{\rm Pei}\approx 0.2$, $\chi_{\rm SS}$ is not divergent near $\delta=0$, where $K_c^{\rm eff} < 1/2$, nor is it divergent near $\delta=1$, where $\Delta_s = 0$. However, $\chi_{\rm SS}$ is divergent for a certain range of moderate δ. Therefore, in these cases, at fixed $T \ll \Delta_s$, $\chi_{\rm SS}$ exhibits a peak as a function of δ at an intermediate value of δ. This peak is shown explicitly in Figs. 2 and 3, where we plot $\bar{\chi}_{\rm SS} \equiv \pi v_F\chi_{\rm SS}$ (thick solid line) versus δ at $T/\omega_0 = 0.1$, for representative parameters. The CDW susceptibility $\bar{\chi}_{\rm CDW} \equiv \pi v_F\chi_{\rm CDW}$ (dashed lines) does not exhibit such a peak.

In Figs. 2 and 3 we also plot Δ_s/ω_0 (thin solid lines), which shows that at low dopings, $\chi_{\rm SS}$ increases with increasing doping, despite the fact that the superconducting pairing strength Δ_s decreases! The reason for this discrepancy is the different doping dependencies of the effective interactions in the charge and spin channels, which determine $K_c^{\rm eff}$ and Δ_s respectively. It is worth mentioning that in the cuprates, the superconducting gap also decreases with increasing doping, which in the underdoped region occurs at the same time that T_c increases!

We now consider an array of weakly coupled quasi-1D chains with dephased CDW, and treat the interchain coupling J on a mean-field level, which means that T_c is determined by the temperature at which $2J\chi_{\rm SS} = 1$ [17, 18]. (The numerical prefactor 2 is determined by the number of nearest neighbor chains.) In this case, T_c exhibits a peak at the same δ where $\chi_{\rm SS}$ is peaked (assuming J is doping independent). The isotope effect exponent α_{T_c} is readily computed [19], and is shown versus δ in Fig. 4 for various values of $\bar{J} \equiv J/(\pi v_F)$. At low dopings, α_{T_c} is larger than the BCS value, then drops below 1/2 as δ is increased. Fig. 4 also shows α_{Δ_s}, which is weakly

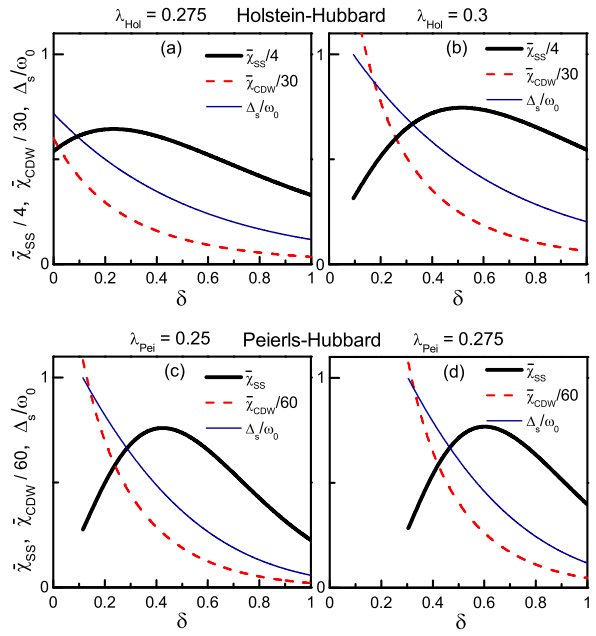

FIG. 3: Doping dependence of $\bar{\chi}_{\rm SS}$ (thick solid lines), $\bar{\chi}_{\rm CDW}$ (dashed lines), and Δ_s/ω_0 (thin solid lines), for the Hol-Hub model (panels a and b), and the Pei-Hub model (panels c and d), both with $\bar{U} = 0.1$ and $E_F/\omega_0 = 5$. $\bar{\chi}_{\rm SS}$ and $\bar{\chi}_{\rm CDW}$ were computed for $T/\omega_0 = 0.1$. The values of $\lambda_{\rm Hol}$ and $\lambda_{\rm Pei}$ are labeled above each plot.

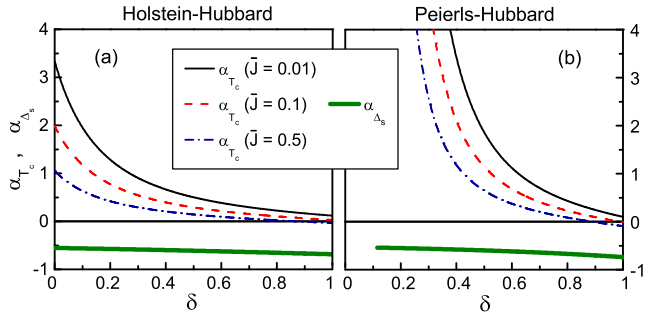

FIG. 4: Dependence of the isotope effect exponents α_{T_c} and α_{Δ_s} on the doping parameter δ and interchain coupling strength $\bar{J}$ for the Hol-Hub model with $\lambda_{\rm Hol} = 0.275$ (panel a) and Pei-Hub model with $\lambda_{\rm Pei} = 0.25$ (panel b). For both panels, $\bar{U} = 0.1$ and $E_F/\omega_0 = 5$. α_{Δ_s} is independent of $\bar{J}$.

doping dependent and negative. Note that there exists a range of δ for which $|\alpha_{T_c}/\alpha_{\Delta_s}| \ll 1$. Similarly, near optimal doping in the cuprates, $|\alpha_{T_c}/\alpha_{T^*}| \ll 1$, where $\alpha_{T^*} = -d\ln T^*/d\ln M < 0$, and T^* is the pseudogap temperature [4].

In some models [17] of high-temperature superconductivity based on stripes [20], the concentration of holes on a stripe remains fixed when the doping in the Cu-O plane changes, but the spacing between the stripes changes. In that case, as the doping increases, the parameter δ remains fixed, but J increases due to the decreased spacing between stripes. Then Fig. 4 predicts that α_{T_c} again decreases with increasing doping. In such a model, in the underdoped region, where the stripes are far apart and represent well defined quasi-1D chains, increasing the doping increases T_c due to the increase in J. But in the overdoped region, the stripes begin to lose their 1D character. This drives T_c down since their quasi-1D character was the reason for the high pairing scale.

To conclude, in the interacting 1DEG, the electron-phonon interaction can cause a strongly divergent superconducting susceptibility with properties that are dramatically different from a Fermi liquid superconductor. Using accurate analytic techniques, we have studied microscopic models of quasi-1D electrons coupled to phonons, and pointed out qualitative similarities to the high-temperature superconductors. These similarities include the doping dependence of T_c, the doping dependence of the superconducting pairing energy, the doping dependence of the isotope effect on T_c, and the sign of the isotope effect on the spin gap.

I would like to acknowledge useful discussions with S. Kivelson. This work was supported by the Department of Energy contract No. DE-FG03-00ER45798.

[1] A. Lanzara *et al.*, Nature (London) **412**, 510 (2001); G.-H. Gweon *et al.*, Nature **430**, 187 (2004).
[2] J.-H. Chung *et al.*, Phys. Rev. B **67**, 014517 (2003).
[3] Isotope effects in the cuprates are reviewed in Guo-meng Zhao *et al.*, J. Phys.: Condens. Matter **13**, R569 (2001).
[4] D. Rubio Temprano *et al.*, Phys. Rev. Lett. **84**, 1990 (2000).
[5] R. Khasanov *et al.*, Phys. Rev. Lett. **92**, 057602 (2004).
[6] For reviews see V. J. Emery, in *Highly Conducting One-Dimensional Solids*, edited by J. T. Devreese, R. P. Evrard, and V. E. van Doren (Plenum, New York, 1979); T. Giamarchi, *Quantum Physics in One Dimension* (Oxford University Press, 2004).
[7] G. T. Zimanyi *et al.*, Phys. Rev. Lett. **60**, 2089 (1988).
[8] J. Voit, Phys. Rev. Lett. **64**, 323 (1990).
[9] I. P. Bindloss, cond-mat/0404154.
[10] I. P. Bindloss and S. A. Kivelson, Phys. Rev. B. (in press).
[11] V. J. Emery *et al.*, Phys. Rev. B **56**, 6120 (1997).
[12] S. A. Kivelson *et al.*, Nature (London) **393**, 550 (1998).
[13] W. P. Su *et al.*, Phys. Rev. Lett. **42**, 1698 (1979).
[14] T. Holstein, Ann. Phys. (NY) **8**, 343 (1959).
[15] A. Luther and V. J. Emery, Phys. Rev. Lett. **33**, 589 (1974).
[16] In the MSRG technique, we approximate the phonon propagator as a step function of frequency (see Ref. 9).
[17] E. W. Carlson *et al.*, Phys. Rev. B **62** 3422 (2000).
[18] E. Arrigoni *et al.*, Phys. Rev. B **69**, 214519 (2004).
[19] We can use $\alpha_{T_c} = -\frac{1}{2}\frac{\Delta T_c/T_c}{\Delta\xi/\xi}$, where $\xi \equiv E_F/\omega_0$, $\Delta\xi$ is infinitesimal, $\Delta T_c \equiv T_c' - T_c$, and T_c' is the transition temperature after changing $l_0 \to l_0' = \ln(\xi + \Delta\xi)$, $c \to c' = c\, l_0/l_0'$, and $\delta \to 1 - c'$. The changes in c and δ ensure that E_F and μ remain fixed when changing $\xi \propto M^{1/2}$.
[20] S. A. Kivelson *et al.*, Rev. Mod. Phys. **75**, 1201 (2003).